~~CONFIDENTIAL~~ RM A7D17

NACA

RESEARCH MEMORANDUM

for the

Bureau of Aeronautics, Navy Department

TESTS OF SUBMERGED DUCT INSTALLATION ON THE RYAN FR-1 AIRPLANE IN THE AMES 40- BY 80-FOOT WIND TUNNEL

By Norman J. Martin

Ames Aeronautical Laboratory
Moffett Field, Calif.

NATIONAL ADVISORY COMMITTEE FOR AERONAUTICS

WASHINGTON

APR 23 1947

~~CONFIDENTIAL~~

NACA RM No. A7D14

NATIONAL ADVISORY COMMITTEE FOR AERONAUTICS

RESEARCH MEMORANDUM

for the

Bureau of Aeronautics, Navy Department

TESTS OF SUBMERGED DUCT INSTALLATION ON THE RYAN FR-1 AIRPLANE IN THE AMES 40- BY 80-FOOT WIND TUNNEL

By Norman J. Martin

SUMMARY

An investigation of an NACA submerged intake installation on the Ryan FR-1 was conducted to determine the full-scale aerodynamic characteristics of this installation. In addition, tests were conducted on the submerged inlet with revised entrance lips and deflectors to determine the configuration which would result in the best dynamic pressure recovery measured at the inlet for this installation without a major rework of the entrance.

Stalling of the air flow over the inner lip surface created excessive dynamic pressure losses with the original entrance. The revised entrance produced a 12-percent increase in dynamic pressure recovery at the design high-speed inlet-velocity ratio and resulted in an improvement of the critical-speed characteristics of the entrance lip. A complete redesign of the entrance including a decrease in ramp angle and adjustment of lip camber is necessary to secure optimum results from this submerged duct installation.

INTRODUCTION

At the request of the Bureau of Aeronautics, Navy Department, an investigation of NACA-type submerged air intakes installed on a Ryan FR-1 airplane was conducted in the Ames 40- by 80-foot wind tunnel. The specific purpose of the investigation was to provide inlet data for application to performance estimates of a modified Ryan FR-1 airplane using these intakes. In addition the investigation

was to serve a more general purpose of providing much needed full-scale information on this type of inlet.

Because of structural requirements, the submerged intakes furnished by the manufacturer deviated considerably from the design recommended as optimum on the basis of small-scale tests (references 1 and 2). The extent of these deviations can be seen in figure 1. These deviations from optimum design reduced considerably the value of the investigation in providing needed full-scale information on flush inlets. The evaluation of the Reynolds number effect also could not be expected to be satisfactory, because the intakes as installed did not correspond exactly to any small-scale installation that had been investigated. The objective of the tests was therefore reduced to an evaluation of the characteristics of one specific full-scale installation plus the effects of minor modifications which could be made on it.

SYMBOLS

α	angle of attack referred to fuselage center line, degrees
C_L	lift coefficient $\left(\frac{L}{qS}\right)$
H	total pressure $[p+q(1+\eta)]$, pounds per square foot
ΔH	loss in total pressure, pounds per square foot
L	lift of airplane, pounds
M	Mach number $\left(\frac{V}{a}\right)$
p	static pressure, pounds per square foot
P	pressure coefficient $\left(\frac{p-p_0}{q_0}\right)$
ρ	mass density of air, slugs per cubic foot
q	dynamic pressure $\left(\frac{1}{2}\rho V^2\right)$, pounds per square foot
S	wing area, square feet
V	velocity, feet per second
a	velocity of sound, feet per second

[redacted]

V_1/V_o inlet-velocity ratio

$1-\Delta H/q_o$ dynamic pressure-recovery coefficient

$(1+\eta)$ compressibility factor $\left(1 + \frac{M^2}{4} + \frac{M^4}{40} + \ldots\right)$

Subscripts

r condition at entrance

o free-stream condition

DESCRIPTION OF MODEL AND APPARATUS

The modified Ryan FR-1 airplane with flush intakes replacing wing leading-edge intakes is a single-place fighter airplane designed to be powered with a Wright R-1820-74 forward engine and a Westinghouse 24-C jet-propulsion engine in the fuselage. A three-view drawing showing the principal dimensions of the airplane is presented in figure 2. The incidence of the wing referred to the airplane reference line is 1°.

Tests of the submerged duct entrance were made with the propeller removed and the jet engine replaced by a variable-speed axial-flow blower. This axial-flow blower provided a means of varying the inlet-velocity ratio from 0.4 to 1.5 (based on a total intake area of 1.47 sq ft) at the free-stream velocity of the tests. The air flowing in the intake system was discharged at the rear of the airplane by means of a tail pipe similar to that existing on the airplane.

Pressure recovery at the entrance was measured by a rake consisting of 189 total-pressure tubes and 38 static-pressure tubes (fig. 3). The total-pressure tubes were connected to an integrating manometer. Static-pressure distribution was obtained by means of flush orifices built into the airplane and connected to water-in-glass manometers. All pressure measurements were recorded photographically.

Modifications were made to the original inlet by rotating the entrance lip outward and changing the deflector length and height. A comparison of the original installation and the final form of the revised lip is shown in figure 4. A photograph of the revised installation is shown in figure 5. The condition of a simulated basic fuselage without submerged ducts was obtained by installing a flush cover plate which effectively sealed these entrances. A photograph of the airplane with the flush cover plate

[redacted]

installed is shown in figure 6. Boundary-layer measurements were made on this simulated basic fuselage by means of three rakes installed at the entrance location, one at the center line of the ramp, one 10 inches above the center line, and one 10 inches below the center line.

TESTS

Tests were first conducted on the simulated basic fuselage to determine the pressure distribution and boundary layer of the basic fuselage at the entrance location to compare with those of small-scale tests. Following these measurements, tests were made on the original submerged entrance to determine values of dynamic pressure recovery at the submerged duct entrance and pressure distribution along the center line of the ramp and over the inner and outer surfaces of the entrance lip. Following the detection of stall along the inner surface of the original lip, a series of developmental tests were made to determine the best lip angle and deflector size for this submerged duct installation. All data were obtained throughout the angle-of-attack range of -2° to 6° and inlet-velocity ratio range of 0.4 to 1.5 at a stream velocity of approximately 100 miles per hour. The design high-speed inlet-velocity ratio is 0.7.

RESULTS AND DISCUSSION

The integrated values of dynamic pressure recoveries at the submerged duct entrance for the original and modified installations are presented in figure 7 for zero angle of attack and are tabulated in table I for other angles of attack. Pressure distributions over the original and modified entrance lips are shown in figure 8. The results of measurements of the boundary layer on the simulated basic fuselage at the entrance location are shown in figure 9. The critical Mach number of the lips (fig. 10) were determined from measured pressure coefficients and computed following the method given in reference 3. Pressure distribution over the basic fuselage and along the center line of the ramp are presented in figure 11 for zero angle of attack. Tabulated values for other angles of attack are presented in table II.

For the original installation the dynamic pressure-recovery characteristics were very unsatisfactory. At zero angle of attack the dynamic pressure recovery was 79 percent at an inlet-velocity ratio of 0.5, 76 percent at an inlet-velocity ratio of 0.7, and 18 percent at an inlet-velocity ratio of 1.5. Small-scale tests (reference 2) have indicated that much higher maximum pressure recoveries and much smaller

decreases in pressure recovery with increases in inlet-velocity ratio can be obtained from installations of this same general type.

An investigation of the pressure distribution over the lip revealed that stall was occurring over the lip inner surface (fig. 8(a)) at approximately the design inlet-velocity ratio of 0.7, thereby preventing a reasonable dynamic pressure recovery (observe difference in pressure distribution between unstalled inner lip at inlet-velocity ratio of 0.6 and stalled lip at inlet-velocity ratio of 0.8). Visual observation of the manometer boards measuring total pressure distribution across the intake confirmed the existence of this stalled condition near the lip inner surface. It was felt that this stalled condition might be due to an unsatisfactory lip shape, lip angle, ramp angle, deflector shape, or a combination of these variables. Because the modified Ryan FR-1 airplane employing these inlets was near the flight-testing stage, it was decided to try to prevent the lip stall by changes not requiring a major rework of the inlets. The modifications were limited, therefore, to lip angle changes and deflector changes.

The first change made to the inlets was to remove the deflectors. This change resulted in no improvement in the dynamic pressure recovery (fig. 7) and stall continued to occur on the inner lip surface at inlet-velocity ratios greater than 0.7. Then, with the deflector reinstalled, the lip angle was changed as shown in figure 4. This change corrected the inner lip stall although peak negative pressures still were located over the inner lip surface. (See lip pressure distributions of fig. 8(b).) The elimination of stall improved the dynamic pressure recovery by 5 percent (from 76 percent to 81 percent) at the design inlet-velocity ratio of 0.7 and resulted in much greater improvement at higher inlet-velocity ratios where stall occurred previously (fig. 7).

With the elimination of lip stall, the next problem was to determine the possibility of raising the general level of the pressure recovery by either further lip angle change or by modification of the deflectors. Since the lip angle had already been changed as much as possible without causing a serious protrusion of the lip outer surface from the fuselage surface, attention was turned to possible modifications of the original deflectors which were as ineffective with the revised lips as with the original lips installed. It was anticipated, from consideration of the results of small-scale tests, that a revision of the deflectors would result in an

improved dynamic pressure recovery. Such was found to be the case. The final form of the revised deflectors improved the pressure recovery an additional 7 percent (from 81.0 percent to 88.0 percent) at an inlet-velocity ratio of 0.7 (fig. 7). However, at inlet-velocities greater than 0.95 the use of the revised deflectors resulted in a decrease in pressure recovery. It was observed that the revised deflectors produced an increase in downflow angle with consequent increase in negative pressure peak values on the lip at inlet-velocity ratios greater than 0.8. The increase in the negative pressure peaks near the leading edge of the entrance lip increased the adverse pressure gradient in the air moving over the lip inner surface. This increased adverse pressure gradient over the lip inner surface tended to produce lip stall and loss in dynamic pressure recovery. The decrease in dynamic pressure recovery with increase in inlet-velocity ratio did not occur in small-scale tests of deflector shapes. However, small-scale tests were made with lower ramp angles and less lip camber and did not exhibit these negative pressure peaks over the lip inner surface. Therefore, it was concluded that if further improvement in pressure recovery is desired a complete rework of the inlets will be necessary, the required rework consisting of a decrease in ramp angle and an adjustment in lip contour to eliminate the high negative pressure peaks on the lip inner surface. With the exception of deflector shape, the reworked inlet would correspond to the inlet originally recommended on the basis of small-scale tests.

Revision of the submerged duct entrance also resulted in an improvement in the critical-speed characteristics of the inlet lip. As first tested, the lips exhibited peak pressures on the inside and of such magnitude that computations indicate that the critical speed would have been exceeded at the design high-speed operating conditions (fig. 10). With the revised entrance the peak pressures were reduced to such an extent that the computed critical speed of the lips remained above the design operating speed as shown in figure 10.

CONCLUSIONS

As the result of tests conducted on a modified Ryan FR-1 airplane with flush intakes replacing wing leading-edge inlets, conclusions were made as follows:

1. Excessive dynamic pressure losses with the original submerged duct entrance resulted from stalling of the air flow over the lip inner surface.

2. A revision to the entrance lip and deflectors resulted in a 12-percent increase in dynamic pressure recovery

at the design inlet-velocity ratio of 0.7 and much larger increases in dynamic pressure recovery at higher inlet-velocity ratios.

3. The modified entrance resulted in an improvement of the critical-speed characteristics of the entrance lips.

4. A complete rework of the entrance including a decrease in ramp angle and adjustment in lip camber is required to secure optimum results from this submerged duct installation.

Ames Aeronautical Laboratory,
National Advisory Committee for Aeronautics,
Moffett Field, Calif.

Approved:

Harry J. Goett,
Aeronautical Engineer.

Norman J. Martin,
Aeronautical Engineer.

REFERENCES

1. Frick, Charles W., Davis, Wallace F., Randall, Lauros H., and Mossman, Emmet A.: An Experimental Investigation of NACA Submerged-Duct Entrances. NACA ACR No. 5I20, 1945.

2. Mossman, Emmet A., and Gault, Donald E.: Development of NACA Submerged Inlets and a Comparison With Wing Leading-Edge Inlets for a 1/4-Scale Model of a Fighter Airplane. NACA CRM No.A7A31, 1947.

3. von Kármán, Th.: Compressibility Effects in Aerodynamics. Jour. Aero. Sci., Vol. 8, No. 9, July 1941, pp. 337-356.

[redacted]

TABLE I.- THE VARIATION OF DYNAMIC PRESSURE RECOVERY WITH THE ANGLE OF ATTACK AND THE INLET-VELOCITY RATIO, PROPELLER REMOVED, RYAN FR-1 AIRPLANE.

Original Installation					
V_1/V_0 \ α	-2	0	2	4	6
0.49	0.570	0.791	0.841	0.785	0.752
.6	.571	.786	.845	.809	.760
.8	.696	.732	.758	.760	.738
1.0	.593	.644	.683	.672	.647
1.25	.405	.467	.498	.506	.486
1.5	.089	.178	.219	.244	.212
Revised Lips and Deflectors					
V_1/V_0 \ α	-2	0	2	4	6
0.4	0.677	0.909	0.927	0.819	0.761
.6	.763	.910	.910	.832	.766
.8	.753	.849	.855	.821	.766
1.0	.707	.780	.809	.790	.738
1.25	.642	.703	.731	.730	.699
1.5	.617	.676	.700	.680	.645

TABLE II.- THE VARIATION OF PRESSURE COEFFICIENT OVER THE BASIC FUSELAGE AND ALONG THE CENTER LINE OF THE RAMP WITH THE ANGLE OF ATTACK AND THE INLET-VELOCITY RATIO, PROPELLER REMOVED, RYAN FR-1 AIRPLANE.

$\alpha = -2^\circ$								
Distance forward lip leading edge (in.)	Inlet-velocity ratio, V_1/V_o							
	0	0.4	0.6	0.8	1.0	1.25	1.5	Basic fuselage
-2	0.387	0.343	0.252	-0.126	-0.568	-1.340	-2.433	0.126
$1\frac{1}{2}$	.430	.279	.231	.042	-.252	-.660	-1.237	.084
$4\frac{1}{2}$	.408	.257	.231	.126	.021	-.206	-.474	.063
$7\frac{1}{2}$	.301	.193	.189	.126	.042	-.103	-.247	.042
$10\frac{1}{2}$	.236	.172	.147	.063	0	-.103	-.186	.021
$13\frac{1}{2}$	.301	.086	.042	-.063	-.110	-.185	-.247	0
$16\frac{1}{2}$	.301	.021	-.063	-.147	-.189	-.268	-.309	0
$19\frac{1}{2}$	.236	-.086	-.147	-.231	-.274	-.330	-.371	0
31	-.107	-.300	-.295	-.336	-.336	-.371	-.392	-.021
$36\frac{1}{2}$	-.129	-.257	-.252	-.294	-.294	-.309	-.309	-.084
$47\frac{1}{2}$	-.172	-.236	-.231	-.063	-.042	-.247	-.268	---
$50\frac{1}{2}$	-.215	-.257	-.274	-.294	-.294	-.289	-.289	---
54	-.279	-.322	-.295	-.316	-.316	-.309	-.309	---
56	-.344	-.364	-.336	-.358	-.358	-.351	-.371	---

TABLE II.- Continued. Ryan FR-1 Airplane.

$\alpha = 0°$								
Distance forward lip leading edge (in.)	Inlet-velocity ratio, V_1/V_o							
	0	0.4	0.6	0.8	1.0	1.25	1.5	Basic fuse-lage
-2	0.547	0.536	0.236	-0.107	-0.548	-1.368	-2.330	0.164
$1\frac{1}{2}$	.610	.408	.236	.042	-.168	-.653	-1.196	.123
$4\frac{1}{2}$	.610	.343	.236	.150	.042	-.189	-.454	.082
$7\frac{1}{2}$	.505	.236	.214	.129	.063	-.105	-.227	.061
$10\frac{1}{2}$	.337	.172	.128	.063	.042	-.105	-.165	.041
$13\frac{1}{2}$	.316	.086	.021	-.063	-.084	-.189	-.247	.020
$16\frac{1}{2}$	.252	-.043	-.107	-.189	-.168	-.253	-.330	.020
$19\frac{1}{2}$	.147	-.129	-.193	-.359	-.252	-.337	-.392	.020
31	-.189	-.322	-.344	-.337	-.316	-.379	-.392	0
$36\frac{1}{2}$	-.189	-.279	-.300	-.295	-.274	-.316	-.309	-.041
$47\frac{1}{2}$	-.211	-.236	-.257	-.252	-.231	-.253	-.247	---
$50\frac{1}{2}$	-.231	-.279	-.279	-.295	-.252	-.274	-.268	---
54	-.273	-.300	-.322	-.316	-.274	-.316	-.309	---
56	-.318	-.343	-.365	-.337	-.316	-.358	-.351	---

TABLE II.- Continued. Ryan FR-1 Airplane.

$\alpha = 2^\circ$								
Distance forward lip leading edge (in.)	Inlet-velocity ratio, V_1/V_0							
	0	0.4	0.6	0.8	1.0	1.25	1.5	Basic fuse-lage
-2	0.568	0.547	0.252	-0.107	-0.569	-1.389	-2.351	0.147
$1\frac{1}{2}$	.610	.421	.252	.086	-.189	-.653	-1.134	.105
$4\frac{1}{2}$	.610	.358	.274	.257	.063	-.189	-.412	.105
$7\frac{1}{2}$	.526	.274	.231	.129	.063	-.105	-.206	.063
$10\frac{1}{2}$	.379	.211	.147	.064	0	-.084	-.144	.042
$13\frac{1}{2}$	.316	.105	.042	-.064	-.106	-.168	-.227	.021
$16\frac{1}{2}$	.274	0	-.084	-.125	-.189	-.232	-.309	.042
$19\frac{1}{2}$	.147	-.105	-.168	-.257	-.294	-.337	-.371	0
31	-.189	-.274	-.316	-.343	-.357	-.379	-.371	0
$36\frac{1}{2}$	-.189	-.232	-.274	-.300	-.294	-.295	-.289	-.042
$47\frac{1}{2}$	-.189	-.211	-.231	-.257	-.252	-.253	-.227	---
$50\frac{1}{2}$	-.232	-.232	-.274	-.279	-.274	-.253	-.268	---
54	-.274	-.274	-.295	-.323	-.316	-.316	-.309	---
56	-.316	-.295	-.366	-.343	-.336	-.337	-.330	---

TABLE II.- Continued. Ryan FR-1 Airplane.

$\alpha = 4^\circ$								
Distance forward lip leading edge (in.)	Inlet-velocity ratio, V_1/V_o							
	0	0.4	0.6	0.8	1.0	1.25	1.5	Basic fuse-lage
-2	0.516	0.463	0.252	-0.086	-0.579	-1.368	-2.351	0.147
$1\frac{1}{2}$	.537	.358	.231	.086	-.193	-.632	-1.093	.105
$4\frac{1}{2}$	.537	.295	.252	.172	.064	-.358	-.392	.063
$7\frac{1}{2}$	.472	.253	.210	.129	.086	-.084	-.186	.063
$10\frac{1}{2}$	.387	.232	.147	.086	.021	-.084	-.144	.042
$13\frac{1}{2}$	.343	.126	.042	-.064	-.107	-.168	-.247	0
$16\frac{1}{2}$	.279	.021	-.084	-.150	-.193	-.274	-.309	.021
$19\frac{1}{2}$	.150	-.105	-.189	-.279	-.300	-.358	-.371	-.021
31	-.193	-.295	-.316	-.343	-.343	-.379	-.371	0
$36\frac{1}{2}$	-.193	-.253	-.274	-.300	-.300	-.316	-.289	-.042
$47\frac{1}{2}$	-.193	-.232	-.252	-.236	-.257	-.253	-.247	---
$50\frac{1}{2}$	-.236	-.253	-.274	-.279	-.279	-.295	-.268	---
54	-.301	-.295	-.316	-.322	-.324	-.337	-.309	---
56	-.322	-.316	-.336	-.343	-.343	-.358	-.330	---

TABLE II.- Concluded. Ryan FR-1 Airplane.

$\alpha = 6^\circ$								
Distance forward lip leading edge (in.)	Inlet-velocity ratio, V_1/V_o							
	0	0.4	0.6	0.8	1.0	1.25	1.5	Basic fuselage
-2	0.451	0.378	0.189	-0.042	-0.579	-1.278	-2.331	0.084
1½	.535	.274	.210	.126	-.172	-.557	-1.073	.063
4½	.535	.253	.252	.210	.086	-.124	-.351	.021
7½	.451	.253	.231	.168	.086	-.041	-.155	.021
10½	.386	.232	.147	.110	.021	-.062	-.144	0
13½	.322	.126	.042	-.042	-.107	-.165	-.248	-.021
16½	.236	0	-.084	-.147	-.214	-.247	-.309	0
19½	.107	-.126	-.189	-.252	-.300	-.330	-.392	-.063
31	-.193	-.295	-.295	-.336	-.343	-.330	-.372	-.021
36½	-.215	-.253	-.274	-.274	-.300	-.289	-.289	-.063
47½	-.236	-.253	-.252	-.252	-.279	-.227	-.247	---
50½	-.258	-.274	-.274	-.252	-.300	-.268	-.268	---
54	-.300	-.316	-.316	-.316	-.322	-.309	-.330	---
56	-.322	-.337	-.336	-.316	-.343	-.330	-.330	---

FIGURE LEGENDS

Figure 1.- Comparison of original and proposed installation of submerged duct entrance on Ryan FR-1 airplane.

Figure 2.- General arrangement of Ryan FR-1 airplane with flush duct installed.

Figure 3.- Submerged duct-entrance rake installed on Ryan FR-1 airplane.

Figure 4.- Comparison of original and revised installation of lips and deflectors on submerged ducts, Ryan FR-1 airplane.

Figure 5.- Revised lip and deflector installation on Ryan FR-1 submerged duct.

Figure 6.- Simulated basic fuselage installation on Ryan FR-1 airplane mounted in the Ames 40- by 80-foot wind tunnel.

Figure 7.- Comparison of entrance dynamic pressure recovery obtained with original installation and with revised lip and deflectors, $\alpha = 0^\circ$, propeller removed, Ryan FR-1 airplane.

Figure 8.- Comparison of pressure coefficient distribution over original lip and revised lip for various inlet-velocity ratios, $\alpha = 0^\circ$, propeller removed, Ryan FR-1 airplane. (a) Original lip.

Figure 8.- Concluded. Ryan FR-1 airplane. (b) Revised lip.

Figure 9.- Boundary layer on simulated basic fuselage at submerged duct entrance location, $\alpha = 0^\circ$, propeller removed, Ryan FR-1 airplane.

Figure 10. Variation of critical Mach number with inlet-velocity ratio for original installation and with revised lip and deflectors, $\alpha = 0^\circ$, Ryan FR-1 airplane.

Figure 11.- Pressure distribution along the center line of the submerged duct ramp for various inlet-velocity ratios, $\alpha = 0^\circ$, propeller removed, Ryan FR-1 airplane.

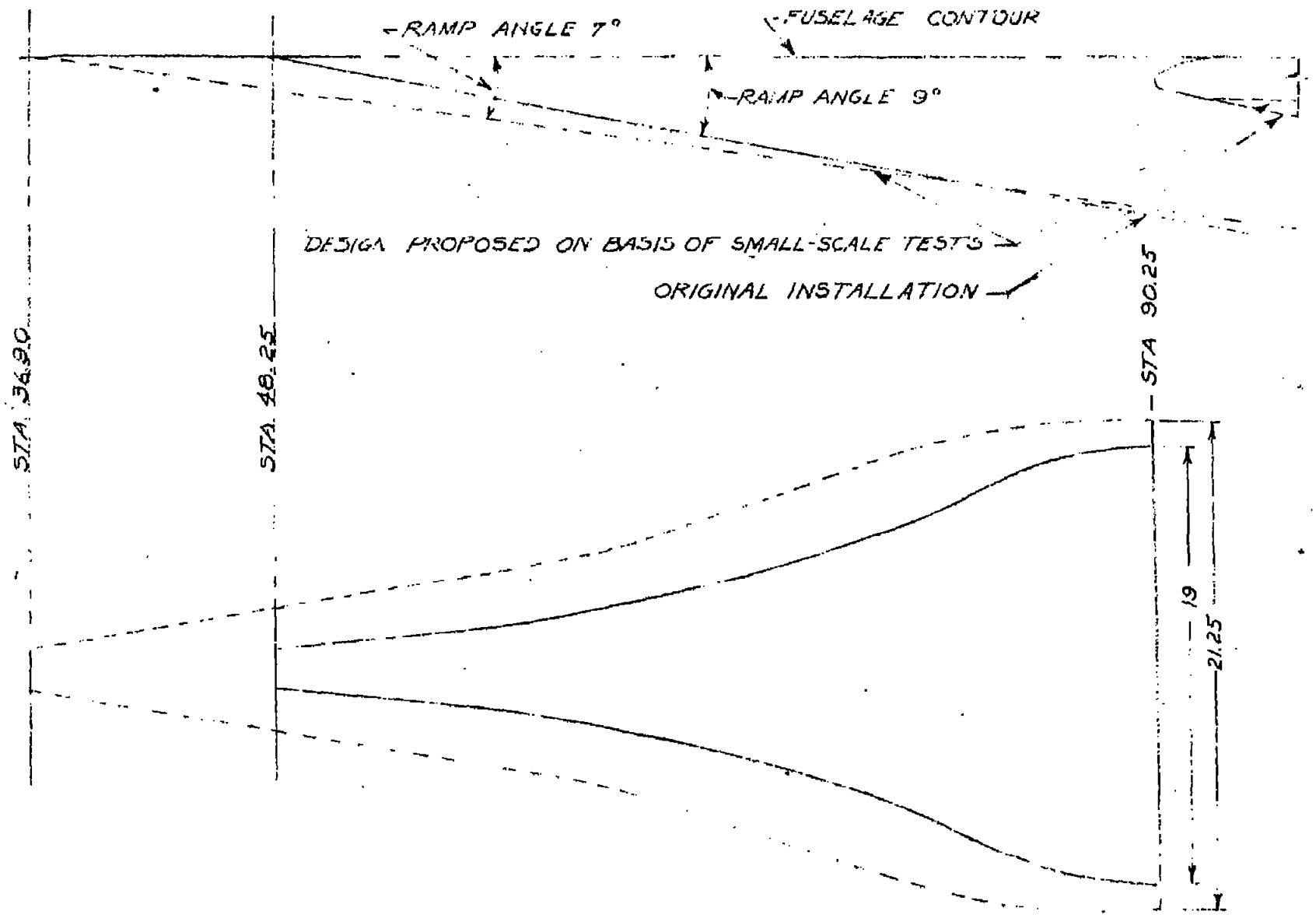

FIGURE 1.- COMPARISON OF ORIGINAL AND PROPOSED INSTALLATION OF SUBMERGED DUCT ENTRANCE ON RYAN FR-1 AIRPLANE.

[redacted]

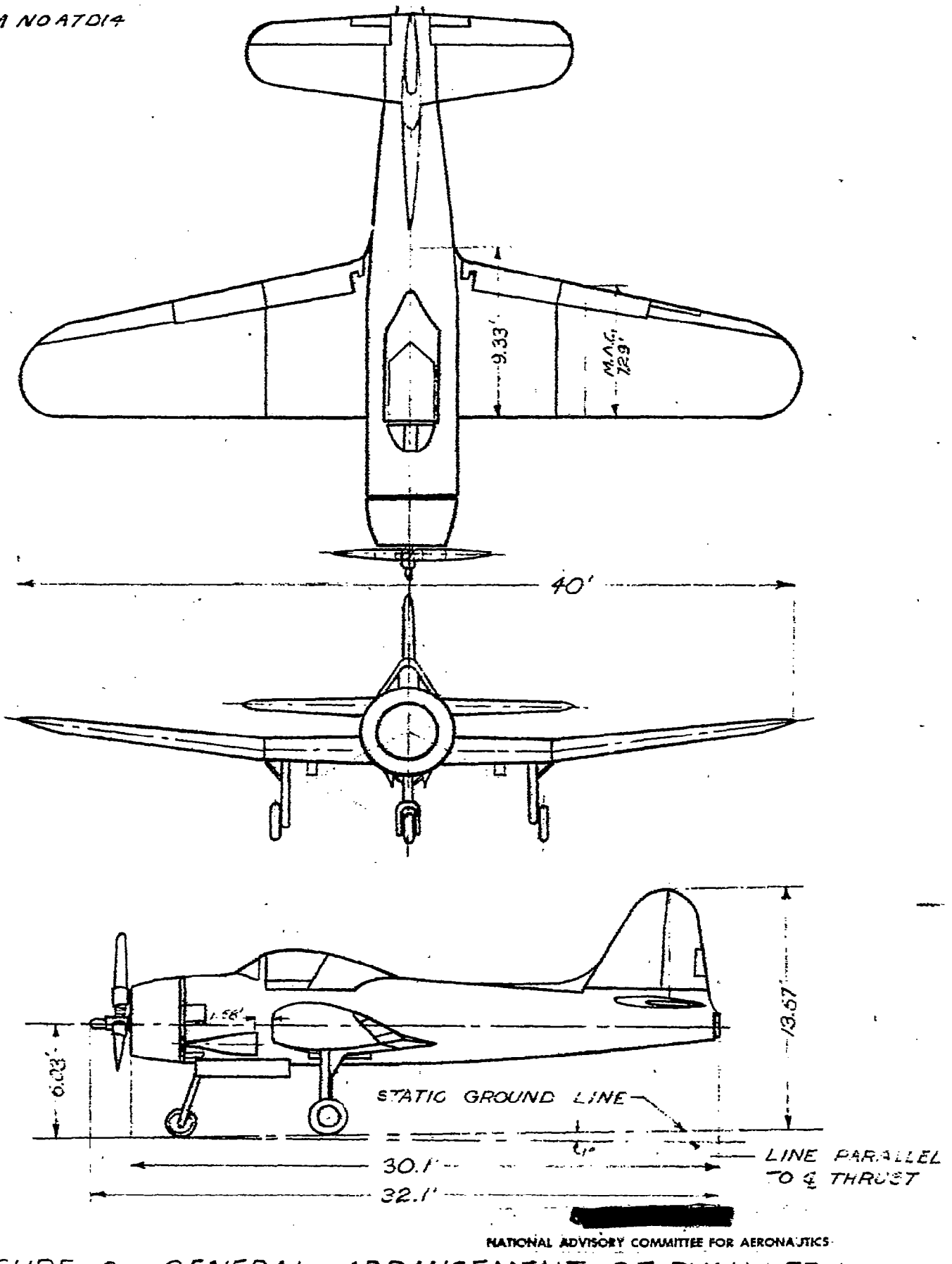

NATIONAL ADVISORY COMMITTEE FOR AERONAUTICS

FIGURE 2 - GENERAL ARRANGEMENT OF RYAN FR-1

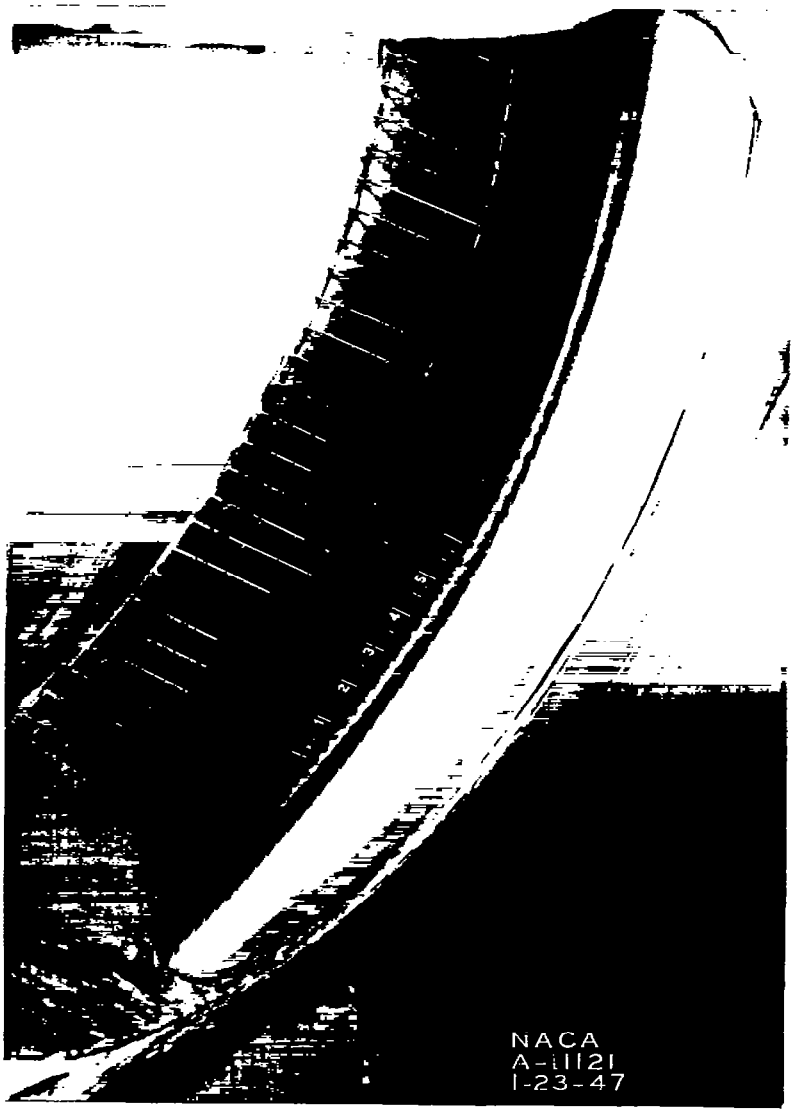

Figure 3.- Submerged duct-entrance rake installed on Ryan FR-1 airplane.

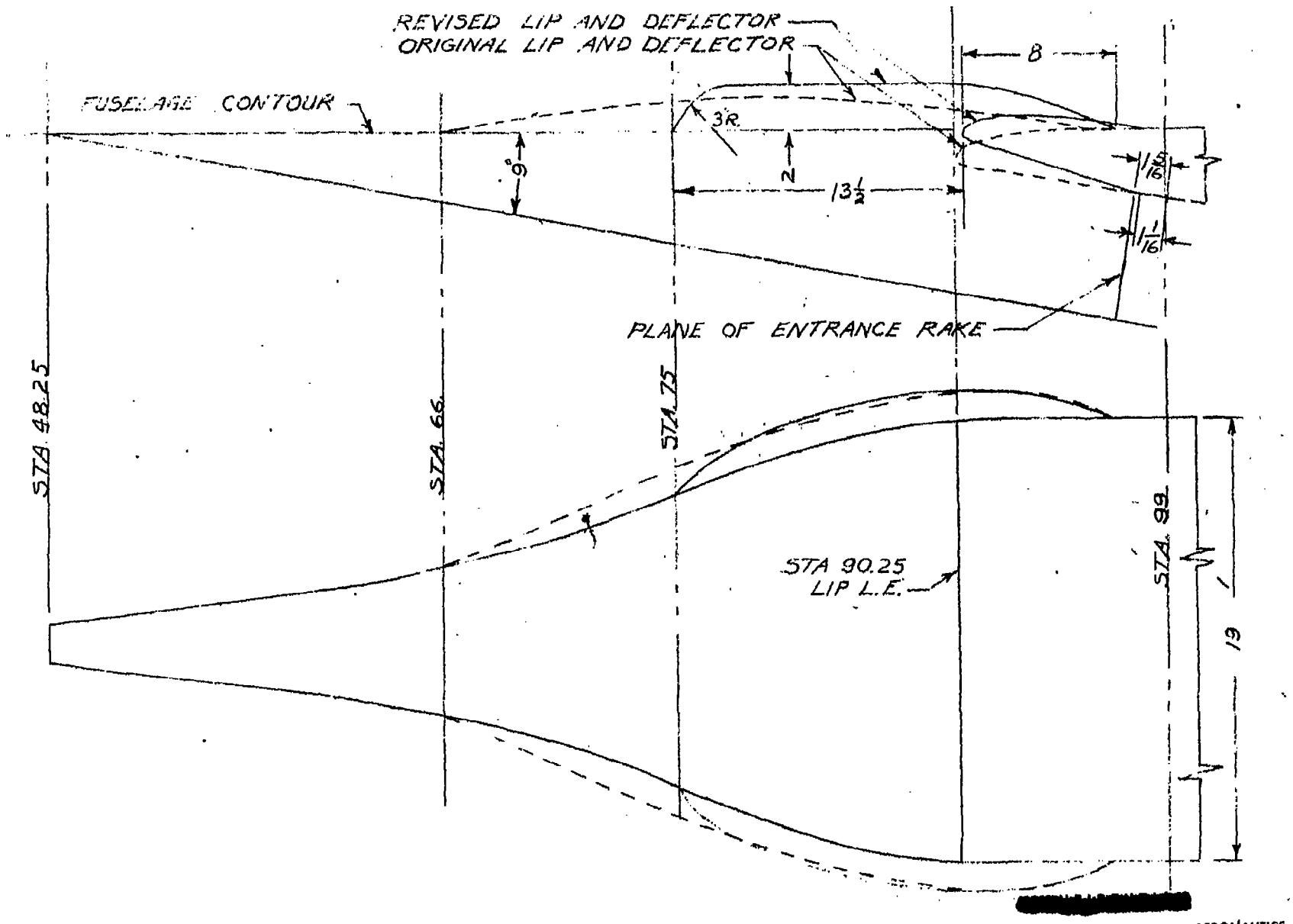

NATIONAL ADVISORY COMMITTEE FOR AERONAUTICS

FIGURE 4.- COMPARISON OF ORIGINAL AND REVISED INSTALLATION OF LIPS AND DEFLECTORS ON SUBMERGED DUCTS. RYAN FR-1 AIRPLANE.

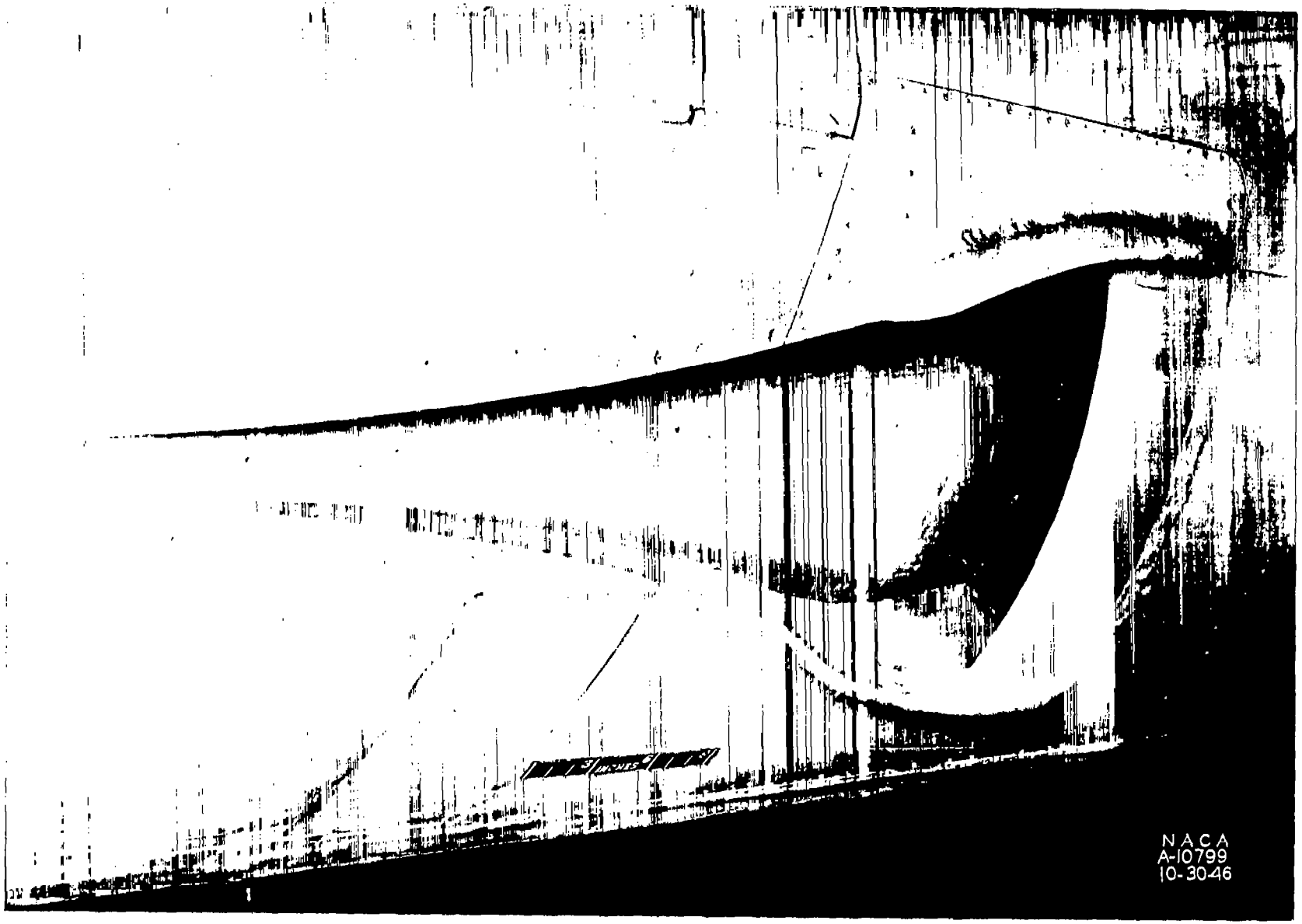

Figure 5.- Revised lip and deflector installation on Ryan FR-1 Submerged Duct.

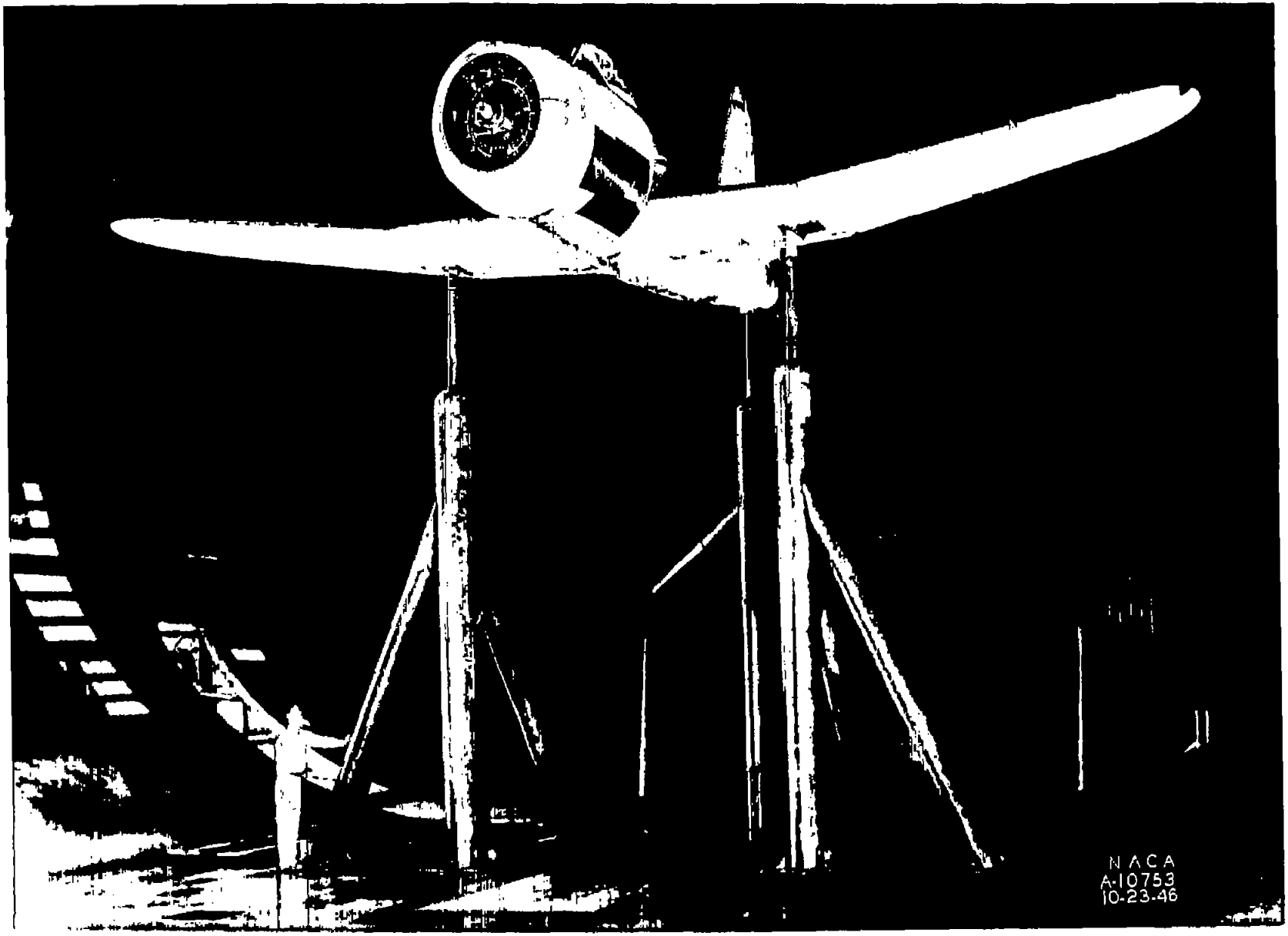

Figure 6.- Simulated basic fuselage installation on Ryan FR-1 airplane mounted in the Ames 40- by 80-foot Wind Tunnel.

[redacted]

NATIONAL ADVISORY COMMITTEE FOR AERONAUTICS
AMES AERONAUTICAL LABORATORY — MOFFETT FIELD, CALIF.

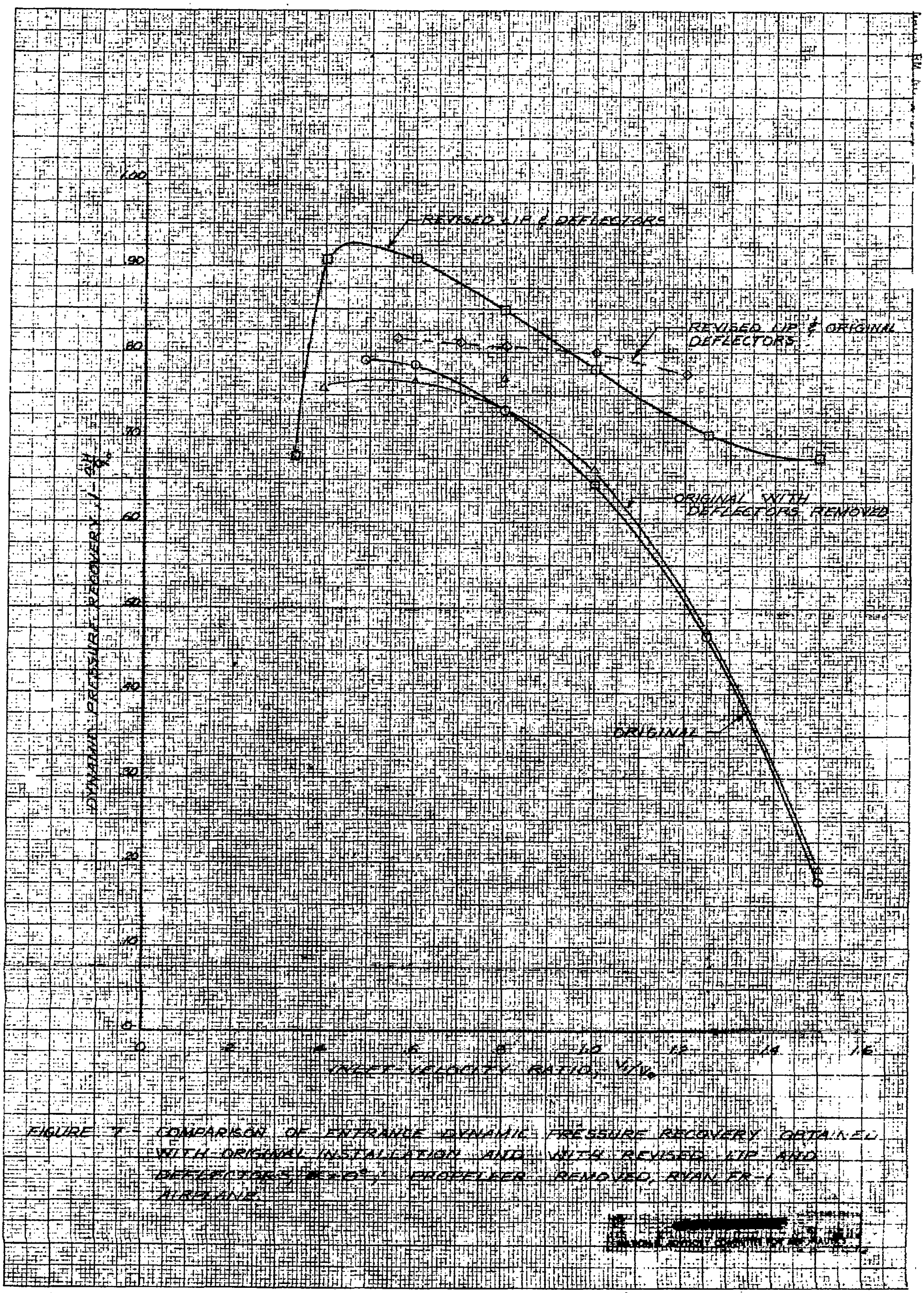

FIGURE 7 - COMPARISON OF ENTRANCE DYNAMIC PRESSURE RECOVERY OBTAINED WITH ORIGINAL INSTALLATION AND WITH REVISED LIP AND DEFLECTORS, $\alpha = 0°$, PROPELLER REMOVED, RYAN FR-1 AIRPLANE.

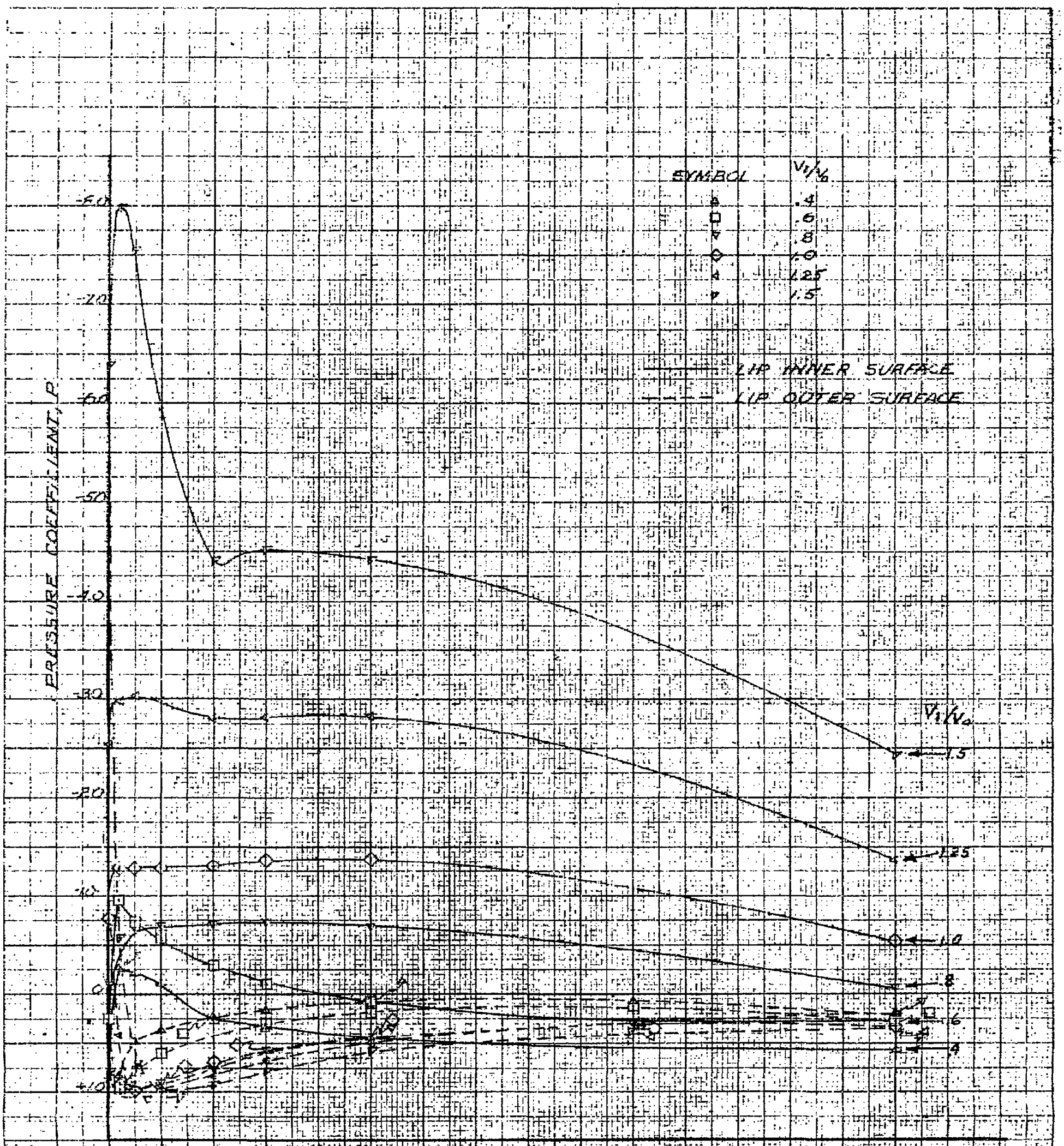

(a) ORIGINAL LIP

FIGURE 8.- COMPARISON OF PRESSURE COEFFICIENT DISTRIBUTION OVER ORIGINAL LIP AND REVISED LIP FOR VARIOUS INLET-VELOCITY RATIOS, $\alpha = 0°$, PROPELLER REMOVED, RYAN FR-1 AIRPLANE.

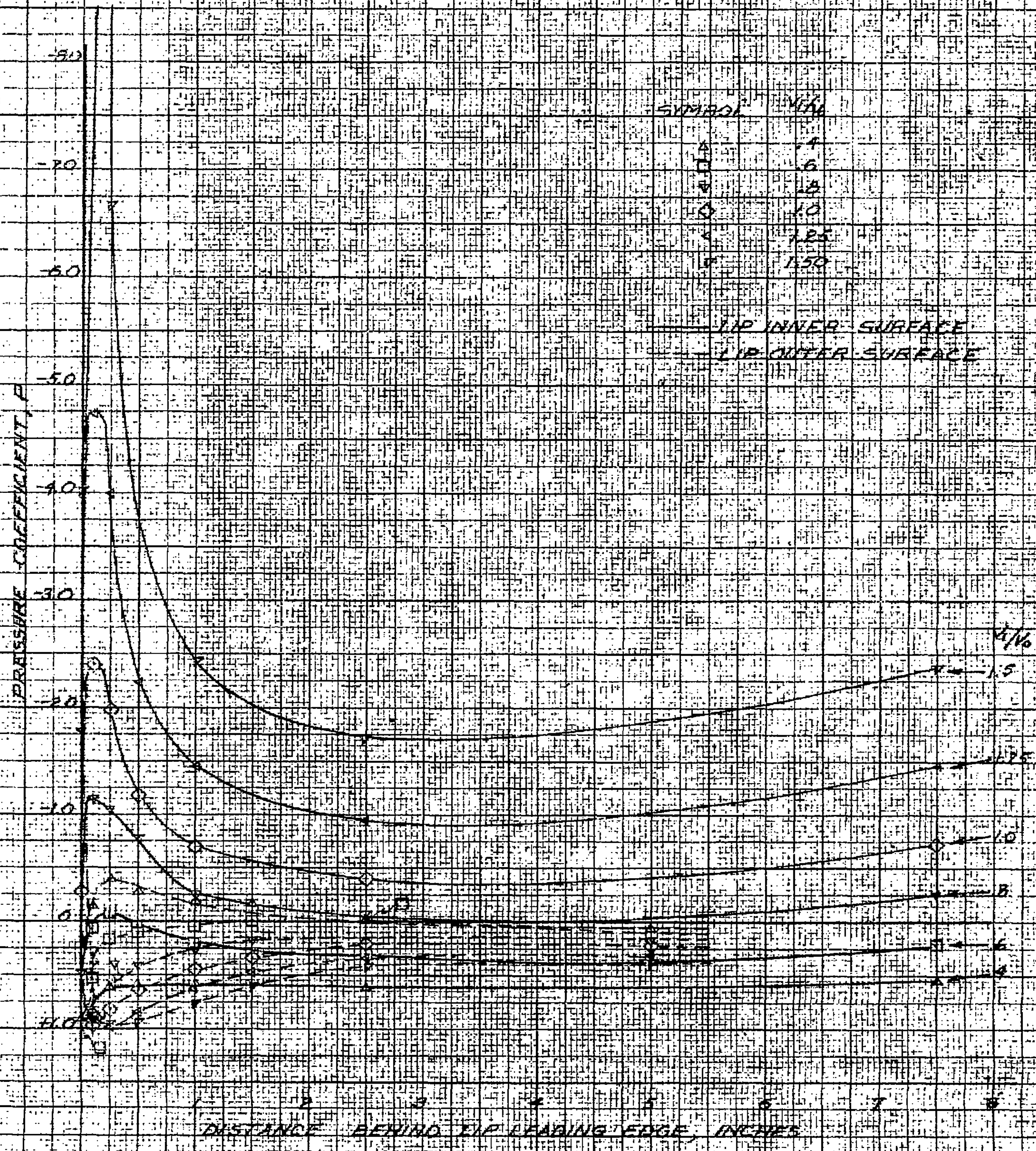

(b) REVISED LIP

FIGURE 8.- CONCLUDED. RYAN FR-1 AIRPLANE

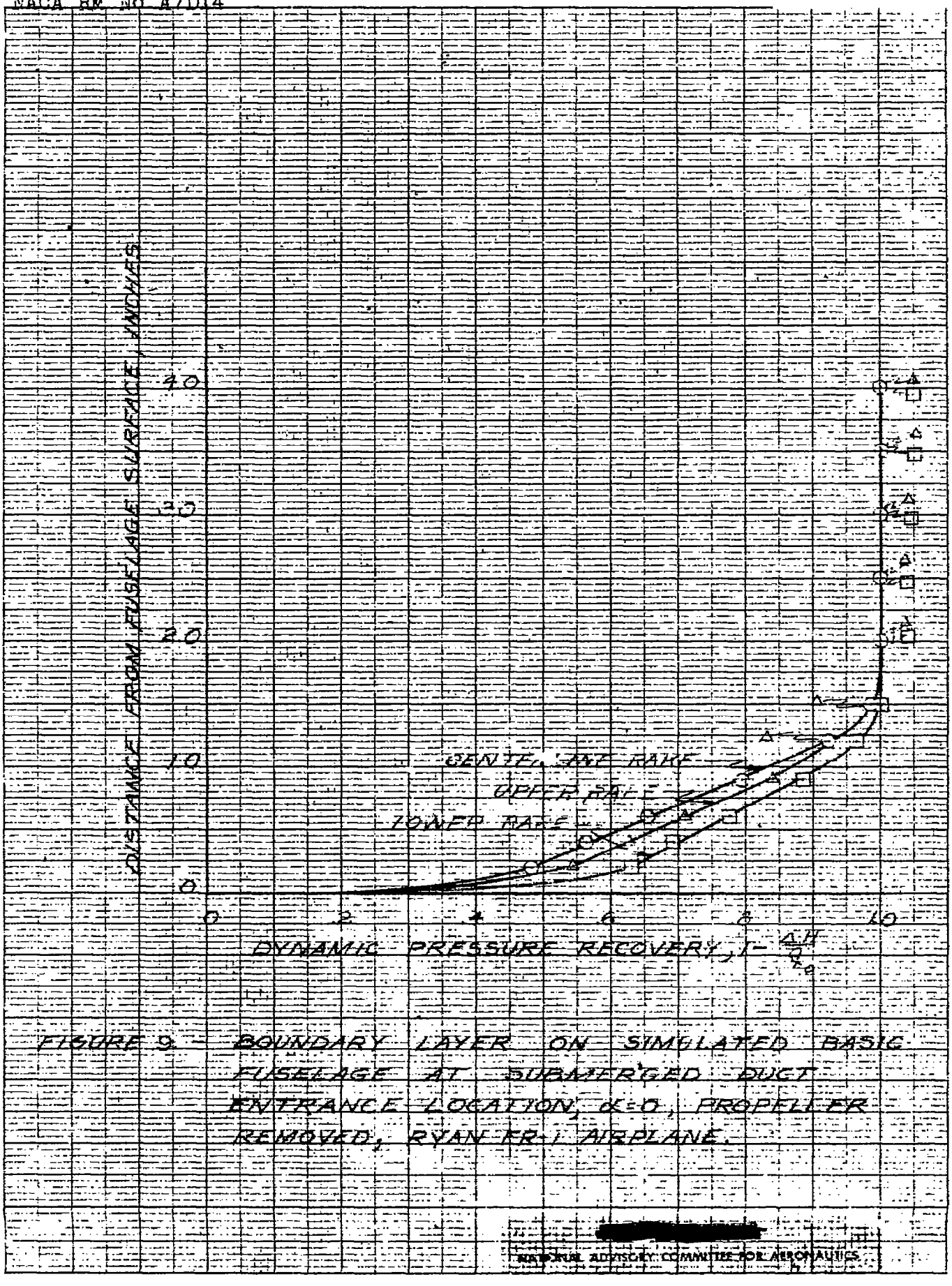

FIGURE 9.- BOUNDARY LAYER ON SIMULATED BASIC FUSELAGE AT SUBMERGED DUCT ENTRANCE LOCATION, $\alpha=0$, PROPELLER REMOVED, RYAN FR-1 AIRPLANE.

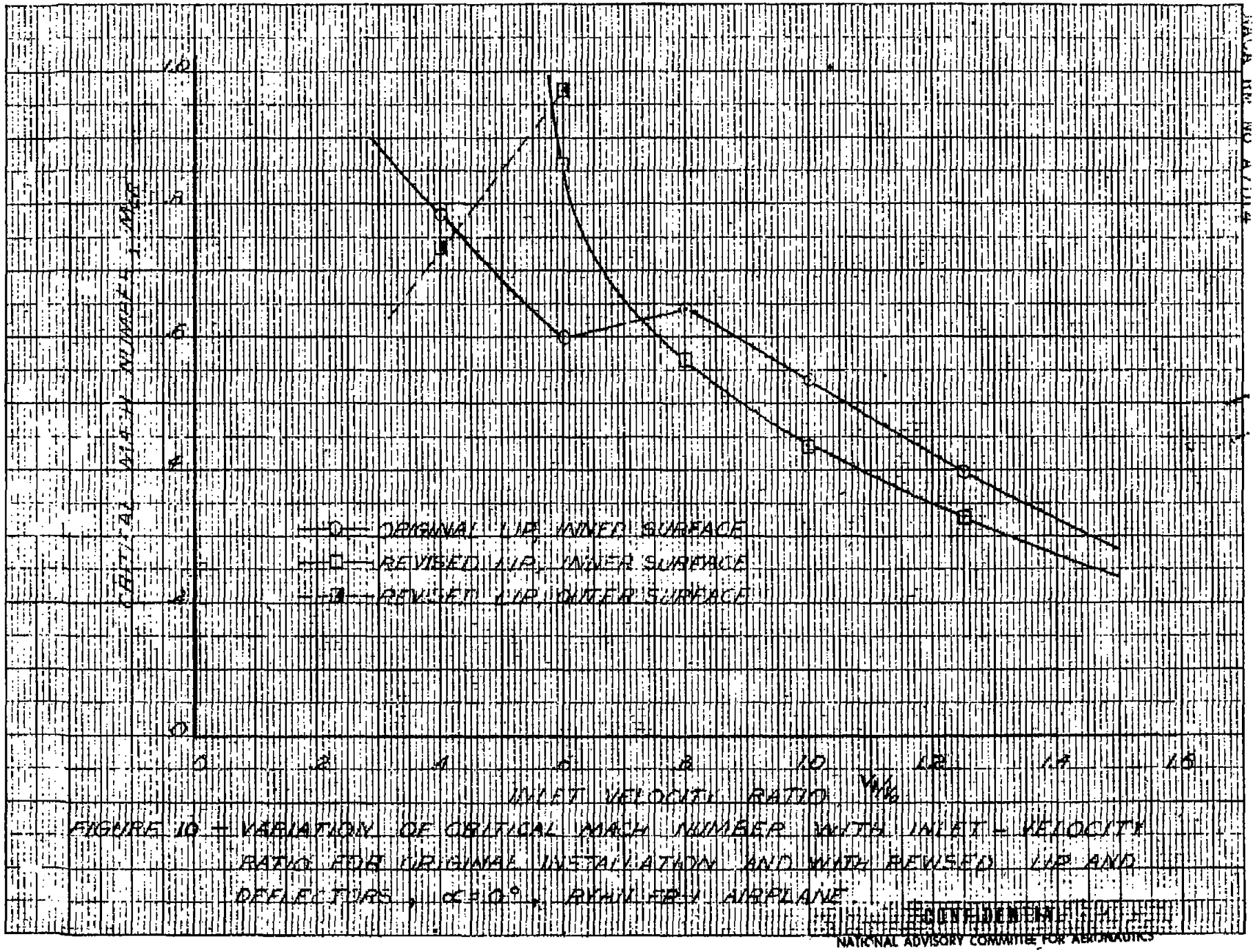

FIGURE 10 - VARIATION OF CRITICAL MACH NUMBER WITH INLET-VELOCITY RATIO FOR ORIGINAL INSTALLATION AND WITH REVISED LIP AND DEFLECTORS, $\alpha = 0°$, RIGHT-HAND AIRPLANE

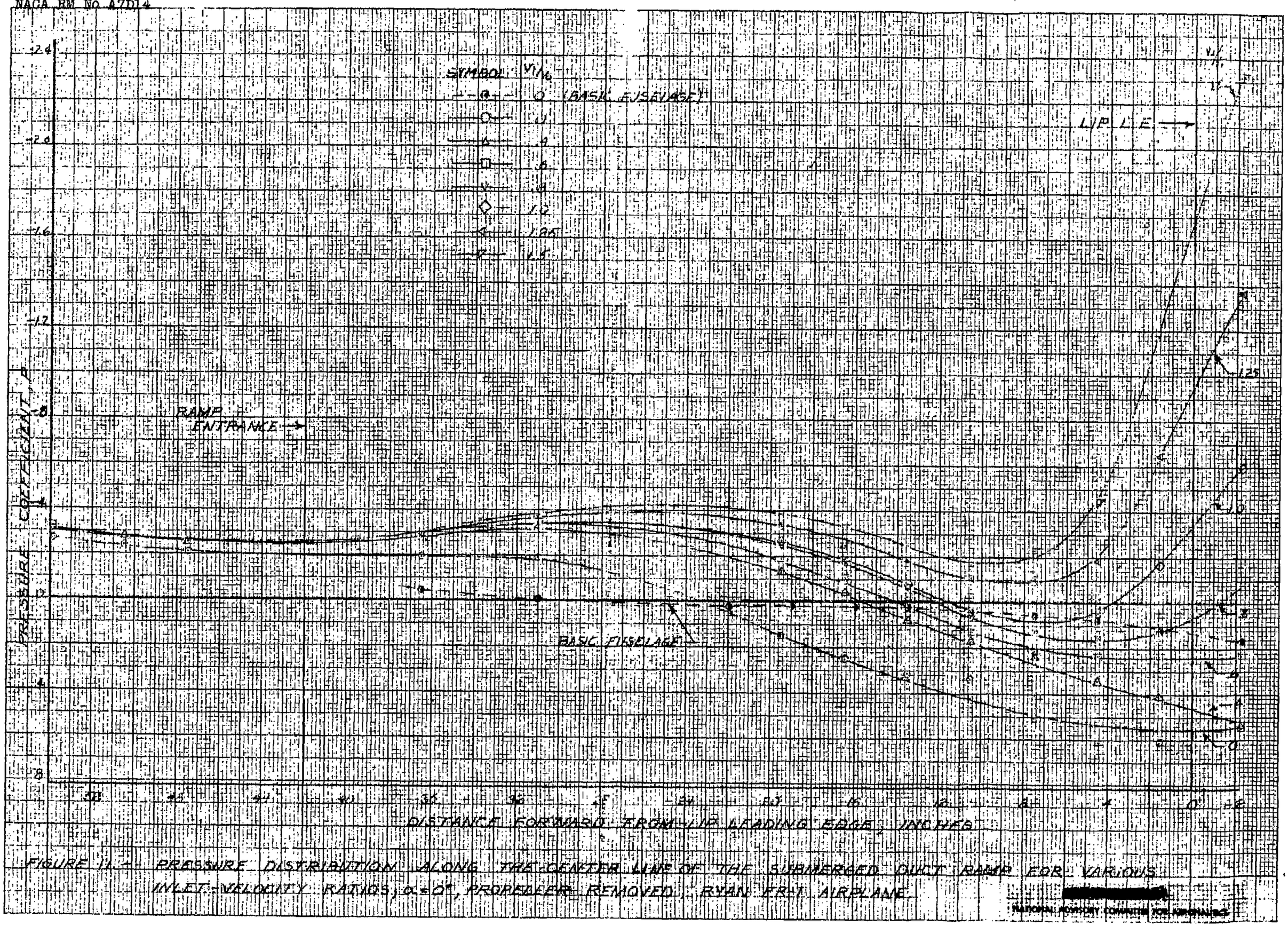

FIGURE 11.- PRESSURE DISTRIBUTION ALONG THE CENTER LINE OF THE SUBMERGED DUCT RAMP FOR VARIOUS INLET-VELOCITY RATIOS, $\alpha = 0°$, PROPELLER REMOVED. RYAN FR-1 AIRPLANE.